Analysis of the Canadian Boreal Forest using Enhanced Resolution ERS-1 Scatterometer Imagery

Clarence J. Wilson III and David G. Long
Brigham Young University
459 CB, Provo, UT 84602
801-378-4884, FAX: 801-378-6586, e-mail: wilsonj@newt.ee.byu.edu

Abstract -- Scatterometer backscatter measurements (σ°) are primarily and traditionally used to estimate wind speed and direction over the ocean. This paper presents an investigation of the backscatter coefficient of boreal forest and neighboring vegetation regions. ERS-1 backscatter $\mathcal{A}$-values of the Canadian boreal forest are imaged using a resolution enhancement algorithm for this analysis. Regions of boreal forest, tundra, and grassland are individually analyzed over the extent of the ERS-1 scatterometer's data set (1992-1995). The annual variation of the mean σ° value for each region is presented. Distinct seasonal variations exist for these vegetation types. Boreal forests exhibit a stronger response (~2.5 dB) during warm summer months than during the snow and ice covered winter months. The results of this study indicate good potential for further analysis of boreal forest regions using ERS-1 scatterometer data.

INTRODUCTION AND BACKGROUND

Boreal forests are found in cool, temperate zones of the northern hemisphere, typically north of the 50^{th} parallel and south of the Arctic Circle. Because they cover such massive regions (~15 million km^2 worldwide), boreal forests are an important factor in understanding the global ecosystem. Boreal forest research has sought to determine how timber resources are being managed, the effects of increasing pollution from modern society (i.e., acid rain and global warming theories), the natural cycles of the forest, and how the forest adapts to change. Remote sensing techniques including aerial photography and SAR imagery have found use in studies requiring infrequent image collection (on the order of years) and studies of small ($<$ 10 km^2) sections of forest. However, as Shubert et al. [1] have suggested, "The processes that control [boreal forest] patterns can change in importance as the space- and time-scales of the pattern of interest are changed." Thus, the understanding of boreal forest cycles over small sections or short time periods does not necessarily apply to the cycles of the forest on macroscopic levels or over long time periods. A means of monitoring the forests on such scales needs to be developed.

Scatterometer σ° Measurements and SIR Imagery

The European Remote Sensing satellite, ERS-1, carries a scatterometer radar which measures the radar backscattering coefficient (σ°) over the entire earth. The primary purpose of this measurement is to determine wind speeds and directions over the ocean; however, backscatter measurements over land surfaces are also useful. Kennett and Li [3, 4] demonstrated that the radar backscatter coefficient values over land are well modeled by the first-order linear function

$$10\, log_{10}\, \sigma^\circ(\theta) = \mathcal{A} + \mathcal{B}\,(\theta - 40^\circ)$$

where θ is the incidence angle of the observation. Such research has demonstrated a strong correlation between $\mathcal{A}$ and $\mathcal{B}$ and vegetation type and surface topology [2, 3, 4].

A major drawback of using spaceborne scatterometer σ° measurements to study vegetation and land surfaces is the coarse resolution of the scatterometer measurements (~50 km for ERS-1). However, spaceborne scatterometers offer the distinct advantages of frequent fly-overs at a wide variety of incidence angles over a period of many years. The ERS-1 scatterometer has provided repeated coverage of the entire world every 4-10 days for over four years. These characteristics make spaceborne scatterometer σ° measurements an attractive resource for studying vegetation on a regional or global scale.

A new resolution enhancement technique, called Scatterometer Image Reconstruction (SIR) [5], has the ability to increase ERS-1 resolution from >50 km/pixel to ~25 km/pixel or better. SIR imagery, along with the frequent coverage of spaceborne scatterometers like ERS-1, can aid in the study of large land regions with ecological significance. This paper investigates the use of enhanced resolution ERS-1 σ° measurement imagery as a technique for studying boreal forests over long time periods and large forest regions.

ANALYSIS OF BOREAL FOREST σ° PATTERNS

The potential of ERS-1 SIR imagery for studying boreal forest regions is investigated by first making imagery of the Canadian boreal forest region from original σ° measurements. Next, subregions of the different vegetation types in the study area are examined over a four year period to investigate interannual backscatter variations.

SIR Imagery

ERS-1 σ° data of the study region (50° N to 70° N, 140° W to 55° W) is grouped into 15-day periods from Jan. 1, 1992 through Oct. 31, 1995 (extent of the available data at press). Each 15-day data group is then processed using the SIR algorithm, producing an 8.9 km/pixel image of the backscatter's $\mathcal{A}$-value average for each 15-day period.

Fig. 1 shows two SIR images thus produced. Fig. 1(a) is the image for February 15-28, 1993. Snow and ice present during this winter period result in a nearly homogeneous backscatter

0-7803-3068-4/96$5.00©1996 IEEE

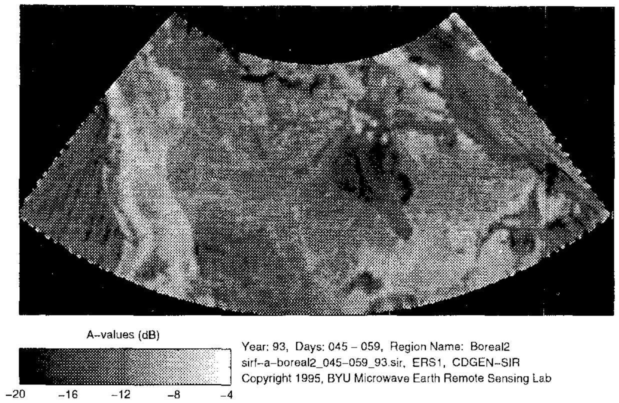

(a) Feb. 15-28, 1993

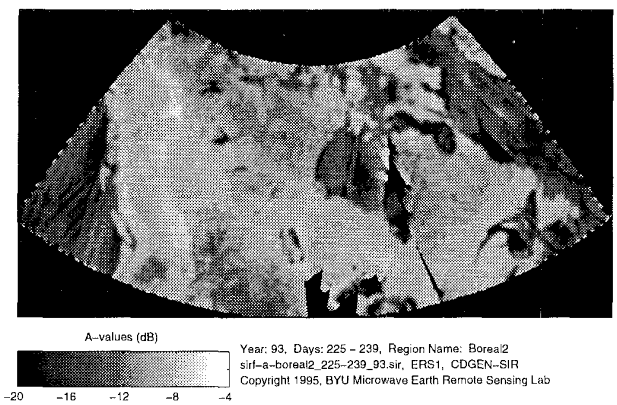

(b) Aug. 15-31, 1993

Figure 1: *SIR Images of Canada. The overall darkness in the upper image is the result of snow and ice coverage. The bright diagonal band in the lower image is the boreal forest.*

$\mathcal{A}$-value with little discrimination among vegetation types. However, several geographic features are still apparent.

Fig. 1(b) shows the region for August 15-31, 1993. Here, a distinctive band that stretches from the northwest to southeast corners of Canada and corresponds to the boreal forest is readily apparent. This image reveals higher contrast levels among the backscatter $\mathcal{A}$-values of the various vegetation types in the region.

One noticeable problem with Fig. 1(b) is the missing image data at the bottom center of the image. The missing data is due to SAR operation on ERS-1 over this area during this time period and is a problem for many of the images produced in this series.

Seasonal Variations

Six subregions of homogeneous vegetation are selected from the Canadian boreal forest and neighboring vegetation types. A map displaying the location of the six subregions is found in Fig. 2. Subregions 1 and 2 are needleleaf evergreen forest (boreal forest); subregions 3 and 4 are lichen woodland; subregion 5 is tundra; and, subregion 6 is grassland/farmland.

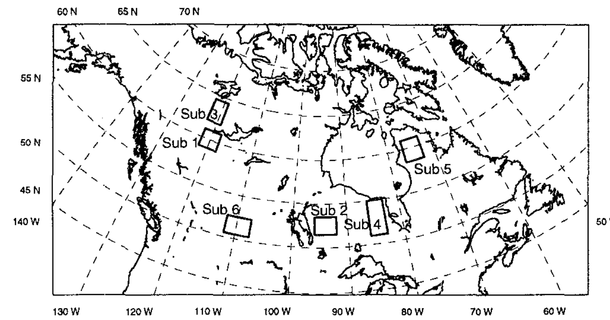

Figure 2: *A map of Canada indicating the six vegetation subregions.*

Fig. 3 is a graph of the mean $\mathcal{A}$-values estimated by the SIR algorithm for the needleleaf evergreen forest subregions (#1 and #2). In these plots, the dashed line represents the weighted average of the $\mathcal{A}$-values from all four years. Portions of the subregions missing data (as discussed above) are not included in calculating such statistics. The backscatter response is 2-3 dB stronger during the summer than the winter. Both plots display a distinctly increasing slope during early spring that climaxes around JD 120 (May 1). This is assumed to represent spring vegetation growth following the melt-off of winter snow and ice. A symmetric feature occurs in the late summer season as the autumn vegetation cycle and winter freezing begins. Note that this occurs earlier for the northern subregion (about JD 260, or mid-September) than the southern subregion (about JD 280, or mid-October).

Fig. 4 is a similar plot for lichen woodland subregions (#3 and #4). Here, again, the spring and autumn vegetation cycles are apparent yielding a 2.5-3 dB difference between winter and summer. The lichen woodland spring and autumn transitions are more rapid than those of the boreal forest. Note that for both vegetation types the northern subregions (#1 and #3) have more abrupt transitions than their southern counterparts.

In Fig. 5 the weighted mean $\mathcal{A}$-values for all six subregions are plotted for comparison. From this figure it is clear that the grassland subregion (#5) backscatter is significantly less than the boreal forests, lichen woodlands, and tundra year-round. The tundra region (#6) backscatter coefficient is less than the boreal forest and lichen woodlands during summer by about 1.5 dB, but during the winter season is approximately the same or slightly greater. It appears the boreal forest and lichen woodland regions all reach a peak in spring around JD 120. However, date of the autumn fall-off varies from region to region. Thus, the seasonal patterns of boreal forests and the surrounding vegetation regions are very pronounced.

CONCLUSION

Study of the boreal forest regions using enhanced resolution imagery produced by the SIR algorithm demonstrates that a dramatic seasonal transition exists for the boreal forest's backscatter coefficient. This annual variation is characterized by a much stronger response (2-3 dB) during the growing

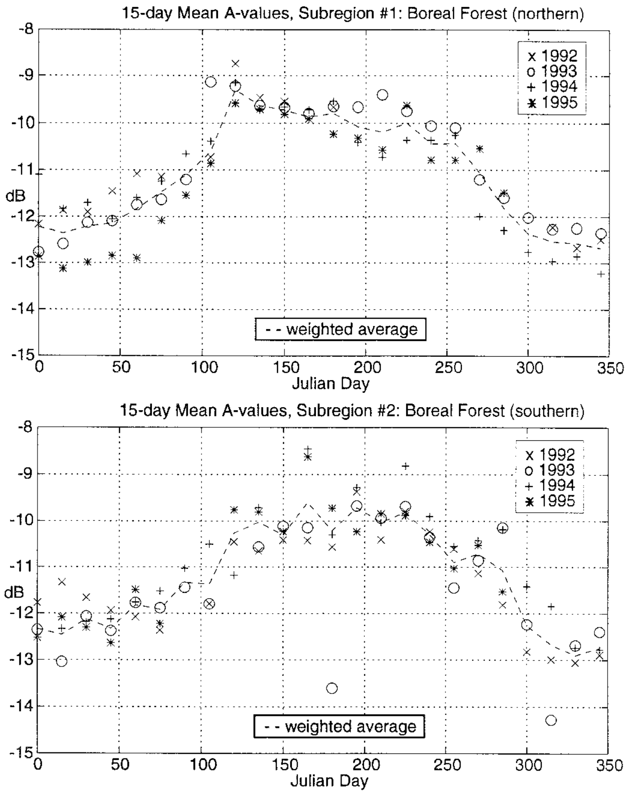

Figure 3: *Mean $\mathcal{A}$-values for subregions 1 and 2 (boreal forest).*

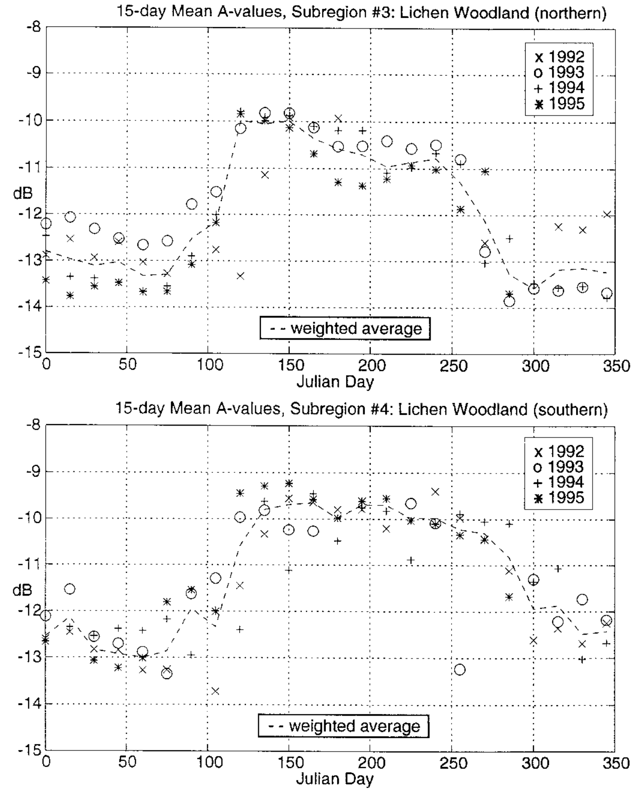

Figure 4: *Mean $\mathcal{A}$-values for subregions 3 and 4 (lichen woodland).*

season throughout the summer than that of the snow and ice covered winter. An even more rapid transition is observed for neighboring lichen woodlands. Tundra has a similar response during winter but differs during summer by about 1.5 dB. Grasslands exhibit a much lower response year-round.

The use of spaceborne scatterometer measurements in combination with SIR image resolution enhancement is a valuable resource for the study of land regions such as boreal forests. With this technique, we have examined the boreal forest on a macroscopic level over several annual cycles. These successful results are substantial motivation for expanded research exploring the use of spaceborne scatterometer backscatter coefficient measurements for the study of boreal forest vegetation regions.

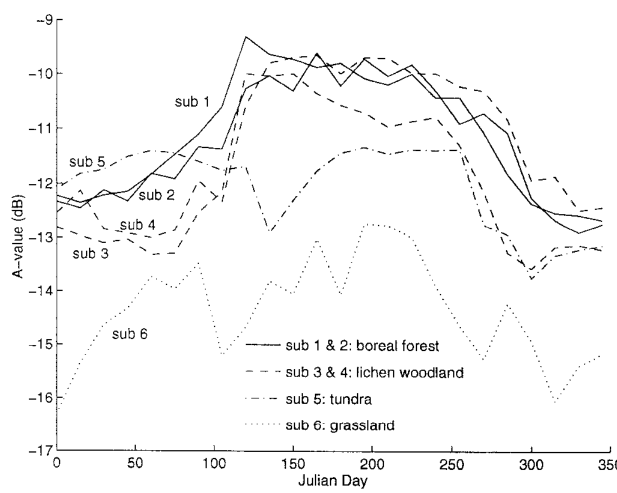

Figure 5: *Weighted Mean $\mathcal{A}$-values over all six subregions*

REFERENCES

[1] H. Shugart, R. Leemans, and G. Bonan, eds., *A Systems Analysis of the Global Boreal Forest.* Cambridge, Great Britain: Cambridge University Press, 1992.

[2] E. Mougin, A. Lopes, P. Frison, and C. Proisy, "Preliminary Analysis of ERS-1 Wind Scatterometer Data over Land Surfaces," *International Journal of Remote Sensing*, vol. 16, no. 2, pp. 391--398, 1995.

[3] R. Kennett and F. Li, "Seasat over Land Scatterometer Data, Part I: Global Overview of the Ku-band Backscatterer Coefficients," *IEEE Trans. Geosc. Rem. Sens.*, vol. 27, pp. 592--605, 1989.

[4] R. Kennett and F. Li, "Seasat over Land Scatterometer Data, Part II: Selection of Extended Area Land-target Sites for the Calibration of Spaceborne Scatterometers," *IEEE Trans. Geosc. Rem. Sens.*, vol. 27, pp. 779--788, 1989.

[5] D. Long, P. Hardin, and P. Whiting, "Resolution Enhancement of Spaceborne Scatterometer Data," *IEEE Trans. Geosc. Rem. Sens.*, vol. 31, pp. 700--715, May 1993.